STEM CELLS AND DEVELOPMENT 17:1185–1194 (2008)

DOI: 10.1089/scd.2008.0028

Non-invasive Longitudinal Tracking of Human Amniotic Fluid Stem Cells in the Mouse Heart

Dawn M. Delo,[1] John Olson,[2] Pedro M. Baptista,[1] Ralph B. D'Agostino Jr.,[3] Anthony Atala,[1] Jian-Ming Zhu,[2] and Shay Soker[1]

Human stem cells from various sources have potential therapeutic applications. The clinical implementation of these therapies introduces the need for methods of noninvasive tracking of cells. The purpose of this study was to evaluate a high resolution magnetic resonance imaging (MRI) technique for in vivo detection and tracking of superparamagnetic micron sized iron oxide particle (MPIO)-labeled human amniotic fluid stem (hAFS) cells injected in the mouse heart. Because of the small subject size, MR signal and resolution of the in vivo MRI were increased using strong gradients, a 7.0 Tesla magnet, and an ECG and respiratory gated gradient echo sequence. MRI images of mouse heart were acquired during a 4 week course of this longitudinal study. At the end of the study, histological analysis was used to correlate cell localization with the MRI results.

Introduction of MPIOs into hAFS had no significant effect upon cell proliferation and differentiation. Results of flow cytometry analysis indicated that hAFS cells remained labeled for up to 4 weeks. MRI of MPIO-labeled hAFS cells injected in agarose gels resulted in significant hypointense regions. Labeled hAFS cells injected into mouse hearts produced hypointense regions in the MR images that could be detected 24 hours and 7, 14, 21 and 28 days post injection. The co-localization of labeled cells within the hypointense regions was confirmed by histological analysis.

These results indicate that high resolution MRI can be used successfully for noninvasive longitudinal tracking of hAFS cells injected in the mouse heart. The potential utility of this finding is that injected stem cells can be tracked in vivo and might serve to monitor cell survival, proliferation and integration into myocardial tissue.

Introduction

Cell transplantation is an intense area of research and appears to be a promising field for cell-based therapy of degenerative diseases. To further enhance the utility of this research, development of methods that track injected cells in vivo would play an important role for identifying the location, survival and cell integration over time. Currently, most cell tracking techniques involve histological analysis, which requires invasive biopsy to evaluate cell integration [1,2]. Thus, there is a need to develop effective noninvasive methods for visualizing transplanted cells.

Presently, there are several available noninvasive imaging methodologies capable of tracking cells in vivo, including radionuclide tomographic imaging, specifically PET (Positron Emission Tomography) and SPECT (Single Positron Emission Computed Tomography), optical imaging, and MRI (Magnetic Resonance Imaging). The radionuclide tomographic imaging methods involve the use of radioactive labeling agents, which have the potential to cause radiation damage to cells. Additionally, the labeling agents used for these methodologies have very short half lives, and therefore labeled cells can be only tracked on the order of only a few days [3–6]. Optical imaging methods, including luminescence and fluorescence, have been used to label stem cells for tracking [7]. These methods rely on the transmission of visible light, which is very susceptible to attenuation in tissue and cannot pass through bone, limiting the use of optical methods to tracking cells that are near the surface of the skin.

In the past few years, the use of MRI for in vivo cell tracking has had significant interest [7–9]. MRI has several

[1]Wake Forest Institute for Regenerative Medicine, [2]Center for Biomolecular Imaging, [3]Department of Biostatistical Sciences, Wake Forest University Health Sciences, Winston-Salem, North Carolina.

advantages: it does not involve the use of radioactive materials; it relies on the transmission of radio frequency energy that can transmit through tissue; it allows repetitive noninvasive tracking of cells in a whole-animal, and detailed depictions of the cells in the organs with near-microscopic anatomic resolution and soft-tissue contrast.

Two classes of materials (gadolinium chelates and iron oxide) are used to label cells for in vivo MRI tracking. Gadolinium provides positive contrast or increases MR signal by shortening the longitudinal relaxation time (T1) and creates a bright signal on a T1-weighted image. However, this approach generally requires a large number of labeled cells to be in a small volume in order to be detectable by MR. Iron oxide provides negative contrast, or decreases MR signal by shortening T2 and T2* relaxation times of protons near the iron and creates a hypointense region on T2 and T2* weighted images. A common criticism of using iron oxide to label cells is the fact that the contrast is negative. For example, there is concern that a hypointense region caused by the presence of an iron oxide labeled cell could be indistinguishable from a hypointense region due to signal decrease caused by anatomy. Still, the ability of iron oxide to affect proton relaxation is significantly greater than that of gadolinium.

Recently, a new iron oxide particle has been investigated for cell tracking by MRI. In 2003, Hinds *et al.* showed that micrometer-sized iron particles (MPIOs) can be used for cellular imaging in vitro and in vivo in developing embryos by MRI [10–12]. The iron oxide can disrupt the magnetic field enough for MRI detectability up to 50 times its size. Further, the coating on MPIOs can include a fluorescent agent, which allows MPIOs to be imaged both by fluorescent microscopy and MRI. Currently, methods for successful MRI monitoring of transplanted stem cells in the heart are quite limited. Some large animal studies have been performed using ultrasmall dextran coated iron oxide particle-labeled mesenchymal stem cells [13,14], but there are very limited studies in smaller animals [15,16], particularly in the heart [17]. The importance of the mouse model is the ability to test non-autologous cell-based cell therapies in genetically modified mice. Further, the use of mice makes it important to successfully track labeled cells in a system with improved spatial resolution.

Recently, a novel source of stem cells from human amniotic fluid (hAFS) has been isolated. These cells are easy to isolate and expand (no feeder layers needed), and are highly expansive (more than 300 population doublings in our experiments thus far). Further, hAFS cells are multipotent (differentiate into representative cell types of all 3 germ layers). As such, these cells represent a potential source for several therapeutic applications [18], thus making it important to find methods for noninvasive tracking of hAFS cells.

In this study, we report that MPIOs can be incorporated into hAFS and imaged by MRI in the mouse heart over 28 days without altering the ability of these cells to multiply or differentiate. The ability to non-invasively track and monitor stem cells in vivo, particularly in the live mouse heart, is of great importance and should open up new possibilities for cellular imaging.

Materials and Methods

hAFS cell labeling

A multipotent subpopulation of progenitor cells present in the human amniotic fluid was isolated as previously described [18]. hAFS cells were plated on non-treated plastic dishes in culture medium consisting of minimum essential alpha-medium, embryonic stem cell certified fetal bovine serum (15%), L-glutamine (1%), antibiotics (1%) (Invitrogen, Carlsbad, California), and Chang Medium® B (18%) and C (2%) (Irvine Scientific, Santa Ana, CA). AFS cells were trypsinized, centrifuged at 1500 RPM, and counted to a density of 1.5×10^6 cells.

The MPIOs (Bangs Laboratories, Fishers, IN) (average size = 1.63 μm) containing magnetite cores encapsulated with styrene/divinyl benzene and coated with dragon green fluorescent dyes (wavelength, 480-nm excitation, 520-nm emission) were used for cell labeling. One million five hundred hAFS cells were mixed with 20 μL of 3×10^8 MPIOs/mL and were incubated for 24 hours. After 24 hours, media was changed and a Zeiss Axiovert 200M fluorescent stereomicroscope was used to confirm the presence of MPIOs in the AFS cells in culture. To determine if the MPIO labeling had any effect on proliferation, we performed a proliferation assay. For this assay, both MPIO-labeled hAFS cells and unlabeled hAFS cells were trypsinized and seeded in a 24-well plate at a density of 8,000 cells/well. Cells were counted at day 1, 2, 3, 4, and 5 in triplicates using a Coulter Counter (Beckman Coulter, Fullerton, CA). This experiment was repeated three times. Counts were plotted for Days 2, 3, 4, and 5 as the percent change for baseline (Day 1) on the raw and the log scale.

To determine the percent incorporation of MPIOs into the cells, and percent labeled over time, flow cytometry analysis was performed. hAFS cells were labeled with MPIOs as described above, using two different doses: 20 μL and 50 μL of 3×10^8 MPIOs particles/mL in order to determine if there are significant differences in MPIO incorporation and labeling efficiency overtime with distinct concentrations. Cells were plated in separate 10 cm tissue culture dishes. Media was changed every 2 days. At 1, 7, 14, 21 and 28 days, cells were trypsinized in triplicates, washed with 1 × Phosphate Buffered Saline (PBS), and analyzed by flow cytometry (Becton Dickinson FACSCalibur) using the FITC channel. The percentage of labeled cells at each time point was determined against the autofluorescence of unlabeled hAFS cells using FlowJo 7.2.2 software from TreeStar, Inc. (Ashland OR, USA).

In vitro MR imaging

Agarose phantoms were made. One percent agarose gels were poured into 15 mL conical tubes. The agarose was allowed to cool until it was viscous. hAFS cells were labeled with MPIOs as described above. After 24 hours, hAFS cells were mixed with 20 μL PBS and injected using a gas tight luer Hamilton syringe (Hamilton Co., Reno, NV) into the slightly cooled agarose and then allowed to further cool slowly at room temperature. Control phantoms were made by injecting only 20 μL PBS. The phantoms were imaged using same

parameters as described in the in Vivo MR Imaging Section below.

hAFS cell differentiation

hAFS cells were labeled with MPIOs as described above. hAFS cells were differentiated into two lineages to confirm multipotentiality after MPIO labeling. The protocols for hAFS cell differentiation were followed as previously published [18]. For adipogenic differentiation, MPIO-labeled hAFS cells were seeded at a density of 3,000 cells/cm^2 and were cultured in DMEM low-glucose medium with 10% FBS, antibiotics (Pen/Strep, Gibco/BRL), and adipogenic supplements (1 mM dexamethasone, 1 mM 3-isobutyl-1-methylxanthine, 10 mg/mL insulin, 60 mM indomethacin (Sigma-Aldrich). For osteogenic differentiation, MPIO labeled hAFS cells were seeded at a density of 3,000 cells/cm^2 and were cultured in DMEM low-glucose medium with 10% FBS (FBS, Gibco/BRL), Pen/Strep and osteogenic supplements (100 nM dexamethasone, 10 mM betaglycerophosphate (Sigma-Aldrich), 0.05 mM ascorbic acid-2-phosphate (Wako Chemicals). Undifferentiated hAFS cells were used as a control for all experiments. To confirm adipogenic differentiation, Oil-Red-O assay was tested at 16 days. To confirm osteogenic differentiation, Alizarin Red assay was tested at 23 days [19].

Cardiac model

All study procedures and imaging protocols were approved by the Wake Forest University Health Sciences Animal Care and Use Committee. The animals had free access to standard diet and water throughout the study. This study involved 4–6 week old male severe combined immuno deficient (SCID-ICR) mice (Taconic, Rockville, MD) (n = 12). Briefly, SCID mice were anesthetized with isoflurane and intubated. The heart was visualized through a midline sternotomy. One million MPIO-labeled hAFS cells were suspended in 20 μL of PBS, and injected into the ventricular wall of the heart using a syringe gas tight luer tip Hamilton syringe. Cells were injected in one or two locations. The incision was closed that the mice monitored postoperatively as outlined in the Institutional Animal care and Use Committee Protocol approved for this study. Additionally, all procedures were performed in accordance with State and Federal Guidelines. Euthanasia was done using methods outline by the American Veterinary Medicine Association.

In vivo MR imaging

All MRI experiments were performed on a 7.0T horizontal magnet small animal scanner (Bruker Biospin Inc., Billerica, MA), with an actively-shielded gradient set capable of a maximum gradient of 400 mT/m. A custom-made Litz volume coil with 25 mm ID (Doty Scientific, Inc, Columbia, SC) was used for both signal transmission and receiving. An ECG and respiration gated FLASH pulse sequence was used for image acquisition with the following parameters: repetition time (TR) = 53.6 ms, echo time (TE) = 2.6 ms, flip angle (FA) = 30 degrees, number of excitations (NEX) = 4, matrix size = 256 × 192, slice thinkness (thk) = 0.60 mm, and field of view (FOV) = 3.0 cm, giving an in-plane resolution of 117 × 156 μm. The respiration and ECG of the mice were monitored (SA Instruments Inc, Stoney Brook, NY). The animals were anesthetized with 3% isoflurane and oxygen at a flow rate of 3 L/min initially, and then maintained with a mixture of 1.5% isoflurane and oxygen at a flow rate of 1 L/min. Mice were imaged at 24 hours, 7, 14, 21, and 28 days. Three of the twelve mice were harvested at 14 days, and 9 mice were harvested at 28 days for histology.

MR image analysis

For characterization of the size and intensity of the hypointense regions surrounding the MPIO-labeled hAFS cells, contiguous MRI slices that covered the entire discernable volume of the hypointense region were analyzed individually. ImageJ (NIH.gov) was used to measure the area of the hypointense region in each slice. The criteria for a pixel to be included in the hypointense area were: the pixel must have an intensity of less than 60% of the average signal intensity of nearby myocardial tissue, the pixel must be located in the region of hypointensity (i.e. pixels that met intensity requirements but were not near the hypointense region were not included) and the pixel must be located inside the myocardial wall. The product of that area and the slice thickness equaled the contribution of that slice to the total volume of the hypointense region. The volumes of the hypointense regions measured ranged from 0.6 mm^3 to 3.4 mm^3. The volumes of the hypointense regions were normalized and set equal to 1 at the first time point. The subsequent volumes were expressed as the absolute volume at that time point divided by the initial absolute volume of that hypointense region.

To quantify the average intensity of a hypointense region, the same contiguous MRI slices covering the entire discernable region of hypointensity were analyzed using ImageJ to determine the average intensity of the area defined to be the hypointense region in each slice as described above. The average intensity was divided by the average intensity of the nearby myocardial wall tissue. This ratio was recorded along with the area of the hypointense region. This procedure was repeated for each slice that included part of the hypointense volume. An average intensity for the entire volume was calculated by multiplying the area of each slice's hypointense region by its average intensity, summing those products, and then dividing by the sum of the areas. To test whether or not the measured values for the volume and intensity would depend on the geometry of the MR slices, long axis and short axis MRI slices of the same hypointense region were obtained during the same scan and analyzed. Measured values of volume and intensity determined from differently oriented slices agreed.

Histology

Histology was performed on mice at 2 (n = 3) and 4 weeks (n = 9) after MRI. Tissues were prepared for cryosectioning by washing them in phosphate-buffered saline and then embedded in embedding medium (Tissue-Tek OCT compound; Miles, Elkhart, NJ), and cryofrozen. The tissues were cryosectioned at 7 μm section thickness in the short axis orientation corresponding to the short axis in vivo

MR images. The sections were immediately stained with 4′, 6-diamidino-2-phenylindole (DAPI) and viewed under fluorescent microscopy for presence of cell-contained MPIOs. Sections were used for Prussian Blue staining to identify the iron in the MPIOs. Further, sections were immunostained to identify human cells using a human specific nuclear matrix antibody (Anti-NuMA) (Calbiochem # NA09L) to prove colocalization of MPIOs with injected AFS cells. In order to do this, the tissues were fixed using 4% Paraformaldehyde, permeabilized, blocked, and incubated with Anti-NuMa for one hour at room temperature. Tissues were washed with Phosphate buffered saline, and incubated with the secondary antibody, TRITC-anti-mouse antibody (Jackson Immuno, West Grove, PA) for 45 minutes. Cells were mounted and viewed using multitrack high resolution confocal microscopy (Zeiss Axiovert 100M). Appropriate negative controls were done in parallel.

Statistical analysis

Statistical analysis was performed using Statistical Analysis Software (SAS). To examine whether the growth rates were different between the labeled and unlabeled groups, we compared the slopes for percent change in growth for each group, relative to their day one values. To do this, we fit an analysis of covariance model, with group as a fixed effect and day as the covariate. We then examined whether there was a group by day interaction which would test whether the slopes were different between groups over time. Using the raw data, the interaction test was nonsignificant ($p > 0.05$). We then examined the model without the interaction to compare the groups for percent change and found no group effect ($p > 0.40$). Since there was evidence that the distribution counts were non-normal on several days (day 3 and 4 in particular), we repeated the analyses on the log scale. Here, we found the percent change (relative to baseline) in each group for each day on the log scale. In these models the group by day interaction was still nonsignficant ($p > 0.14$), and the main effect for group (when the interaction was removed from the mode) was also non-significant ($p > 0.16$). These analyses suggest that there is no statistical evidence that there is a significant difference in growth rates between groups on the raw (or log) scales and that the over all counts were similar across days (on the raw and log scale).

For the flow cytometry analysis, statistical analysis of the data was done using two tailed and two-sample equal variance Student's t-tests. Statistical significance was set at the 95% confidence level. Data are presented as the mean ± standard error of the mean.

Results

Cell labeling

MPIO particles were successfully introduced into hAFS cells. Twenty-four hours after labeling, the cells were visualized by fluorescence microscopy to confirm the presence of MPIOs in the hAFS cells (Fig. 1A, B). Agarose phantoms were prepared by injecting 1 million MPIO-labeled hAFS, and imaged by MRI. Phantoms of labeled cells had hypointense regions in several adjacent slices detectable by MRI. Phantoms injected with PBS had no hypointense regions. Representative axial images of the labeled and PBS injected phantoms are shown (Fig. 1C, D).

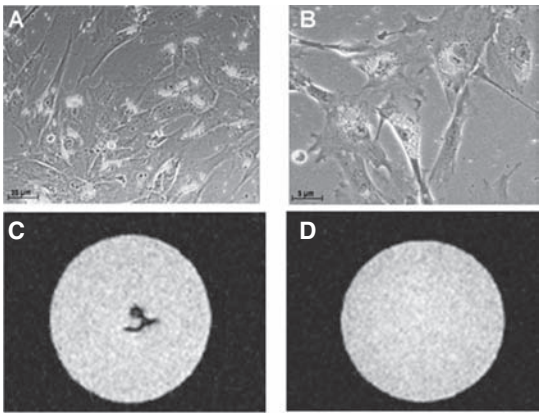

FIG. 1. MPIO labeling of human amniotic fluid stem cells. Cells were imaged by fluorescence microscopy to confirm successful incorporation of the MPIOs in the cells (**A** and **B**). Agarose phantoms were made by injecting 1.5×10^6 MPIO labeled stem cells into 1% agarose in conical tubes and imaged by MRI. A clear hypointense region where the labeled stem cells were injected was imaged successfully by MRI (**C**). The control phantom demonstrated no hypointense region (**D**).

In vitro analysis of MPIO-labeled AFS cells

Cell numbers were determined after 1, 2, 3, 4, and 5 days. The numbers were plotted as a function of percent growth relative to the cell count at day 1 (Fig. 2). The results of proliferation assays indicated that the ability of AFS to divide was not affected by MPIO labeling.

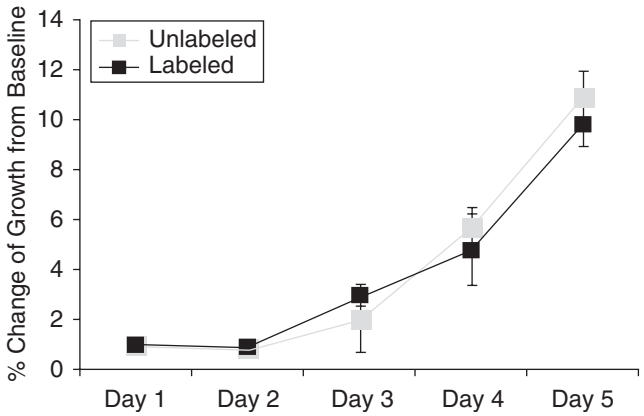

FIG. 2. Proliferation analysis of MPIOs-labeled hAFS cells. 8,000 hAFS cells were plated in each well of a 24 well plate. Cells were counted in triplicates using a Coulter Counter after 1, 2, 3, 4, and 5 days. Counts were plotted as a function of percent change in growth relative to Day 1. Results demonstrated that the labeled stem cells do not differ in proliferation from the unlabeled stem cells.

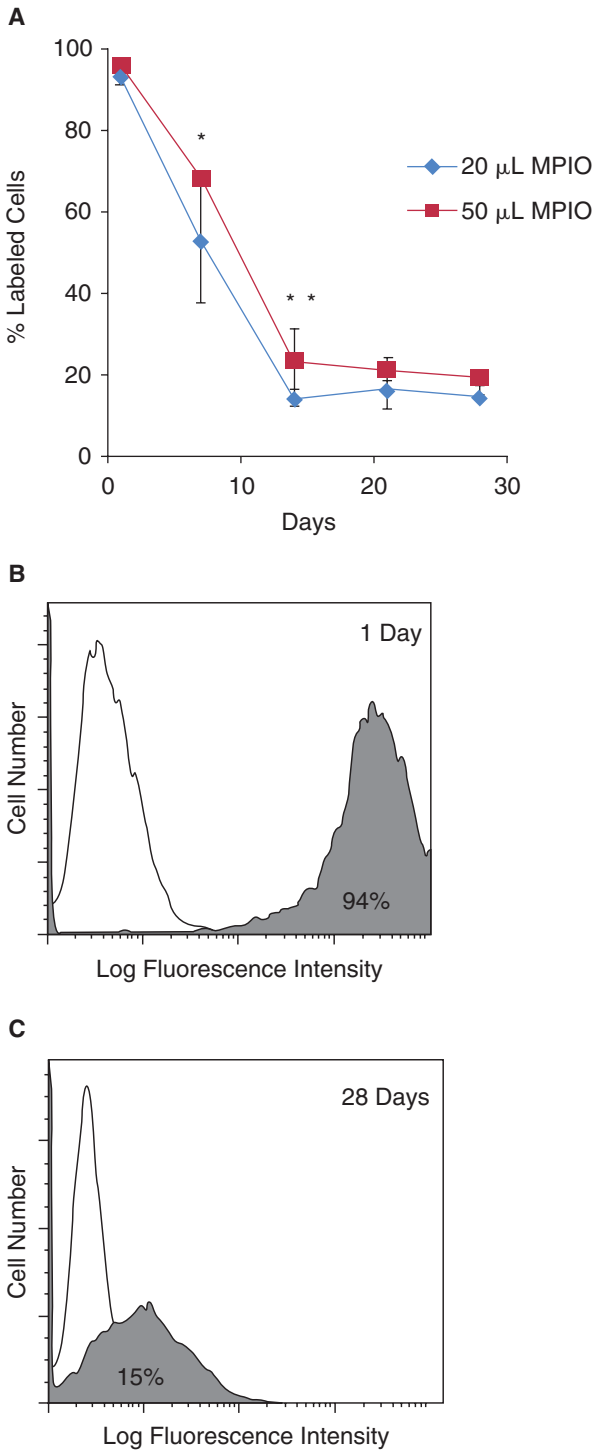

FIG. 3. Time course analysis of MPIO-labeled hAFS cells. The percentage of labeled hAFS cells was determined by flow cytometry at several time points up to 28 days after labeling (**A**). There are statistically significant differences at 7 and 14 days (*$p = 0.0213$ and **$p = 0.0095$, respectively), but at 21 and 28 days there are no statistical differences ($p > 0.05$) between the two used doses of MPIOs. Histograms (**B** and **C**) represent the distribution of labeled hAFS cells with 20 μL of MPIOs compared with unlabeled AFS cells after 24 hours and 28 days, respectively.

To track the stem cells in vivo, it was important that they remained labeled over a number of cell divisions. In vitro studies were done to determine the labeling decline over time. Cells were analyzed by flow cytometry after 24 hours, 7, 14, 21 and 28 days. The hAFS cells labeled with 50 ul of MPIOs displayed a higher percentage of labeled cells over time than the cells labeled with only 20 ul of particles. At 1, 21 and 28 days there were no statistical differences ($p > 0.05$) between the two used doses of MPIOs (Fig. 3A). Thus, the lower dose of MPIOs was sufficient to efficiently label (94%) and maintain labeled a significant percentage of hAFS cells up to 4 weeks (15%) in vitro (Fig. 3B, C).

To test that MPIO labeling of AFS cells does not affect multipotentiality, cells were analyzed for adipogenic and osteogenic differentiation following previously established protocols [18]. Results indicated that both unlabeled and MPIO-labeled hAFS cells maintained their ability to differentiate into adipogenic (Fig. 4A, B) and osteogenic (Fig. 4C, D) lineages.

In vivo MRI studies

To show that labeled stem cells could be imaged longitudinally, we imaged the hearts of mice in vivo 1, 2 and 4 weeks post injection. The time-course of imaging done on hearts after injection is shown in Figures 5 and 6. Representative MRI images taken of the injected hearts after 1, 2, and 4 weeks are shown in both the short and long axis orientation. These images show clear hypointense regions at the location of the injections (Fig. 5A–F). Quantification of the size/volume of the hypointense regions of the mice injected with labeled stem cells showed that the measured volumes of the hypointense region associated with the labeled cells did not change significantly during the 4 weeks of the study (Fig. 6A).

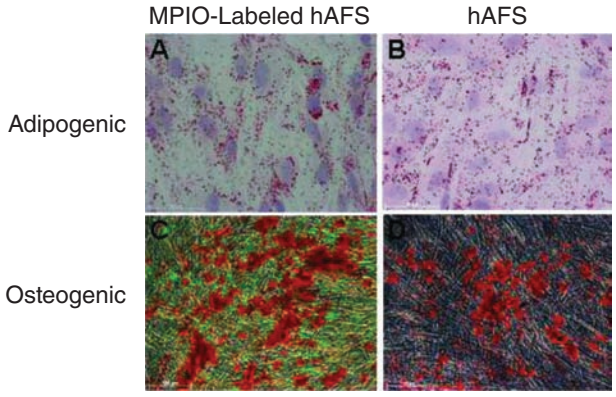

FIG. 4. Lineage differentiation of MPIO-labeled hAFS cells. The multipotentiality of MPIO-labeled hAFS cells was confirmed after adipogenic and osteogenic differentiation. After 16 days of adipogenic differentiation, MPIO-labeled hAFS cells were analyzed by Oil-Red-O assay demonstrating presence of lipid vacuoles in the differentiated MPIO-labeled hAFS cells. After 23 days of osteogenic differentiation, cells were analyzed by Alizarin Red Assay demonstrating presence of calcium production in the differentiated MPIO-labeled hAFS cells.

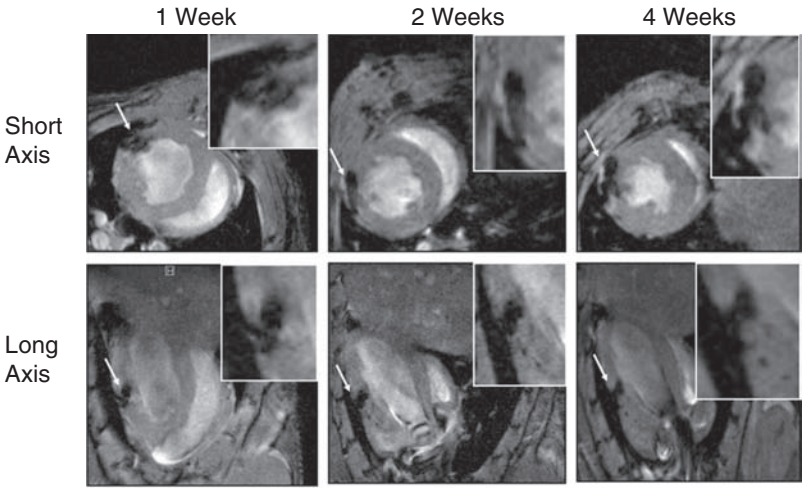

FIG. 5. MPIO-labeled cells are detectd in the live mouse heart by MRI. One million cells were injected in one location in the mouse heart. Multiple mice ($n = 6$) were imaged by MRI at the short and long axis images after 1 day and after 1, 2, and 4 weeks, as indicated. In all scans, significant hypointense regions are seen in the location of the MPIO-labeled hAFS cell injection sites. Size and intensity remains essentially unchanged.

Quantification of the average intensity of the hypointense regions over time of the mice showed that the average intensity of the hypointense regions did not change significantly during the 4 weeks of the study (Fig. 6B). The hearts were harvested and examined histologically to precisely localize the injected MPIO-labeled AFS cell. Cells were injected in two locations and are confirmed by MR imaging of the two hypointense regions (Fig. 7A, arrows) in the wall of the left ventricle. Hypointense regions can be seen where the MPIO-labeled hAFS cells were injected. Immediately after MRI, the mice were euthanized and the heart analyzed by histology to confirm that the signal is due to the MPIOs incorporated into the heart. The heart was embedded, apex down, in order to match sections to the short axis slices of the MRI. Frozen sections were stained with the nuclear stain DAPI and imaged by fluorescent microscopy to view the MPIO-labeled hAFS cells in the heart (Fig. 7B, C). The locations of the fluorescent MPIO-labeled hAFS cells in the heart closely match the location of the hypointense regions from the MRI images. Sections were further stained using Prussian blue and Nuclear red counterstaining (Fig. 7D, 7E). The locations of Prussian blue iron staining similarly correspond to the location of the fluorescent particles and the hypointense regions seen during MRI imaging. Further, we stained hAFS cells for a human specific marker, human specific nuclear matrix antibody (Anti-NuMA) and analyzed by confocal microscopy (Fig. 7F), indicated that the hAFS maintain labeled in vivo. results were obtained for all timepoints (not shown). Together the results confirm that hypointense regions seen by MRI are the MPIO-labeled hAFS stem cells injected into the mouse heart.

Discussion

This study describes the in vivo MRI identification and tracking of MPIO-labeled hAFS cells in the mouse heart over time. The major findings of this study are that: 1) hAFS cells can be labeled with MPIOs; 2) labeling does not interfere with the ability of the hAFS cells to proliferate or differentiate; 3) ECG and respiratory gating produces MRI images of mouse heart that contain clearly defined areas of hypointensity; and 4) MPIO-labeled hAFS cells can be tracked in vivo for at least 4 week post injection without loss of image intensity or volume.

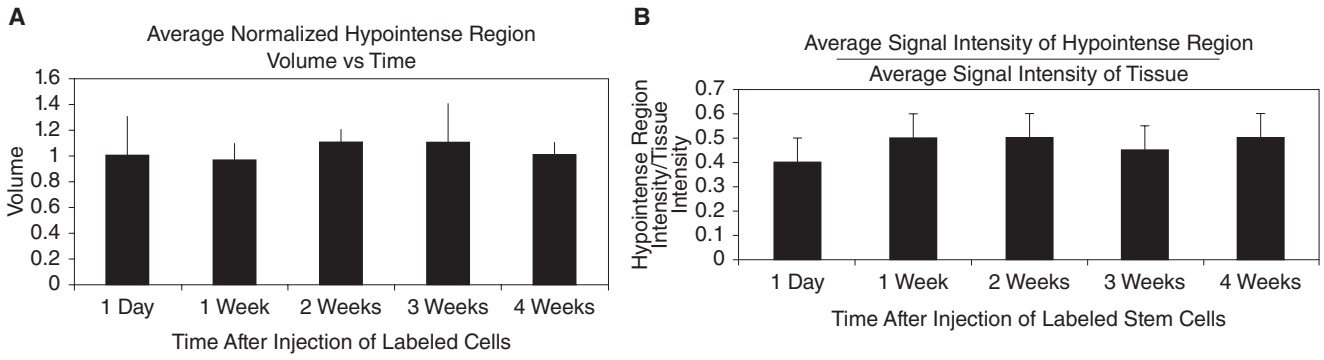

FIG. 6. Quantification of the hypointense region. (**A**) Depicts the average of the normalized hypointense region volume over time. The average normalized hypointense region volume remained unchanged for the duration of the study. (**B**) Depicts the average signal intensity of the hypointense region/tissue intensity over time. The average signal intensity of the hypointense regions remained unchanged for the duration of the study.

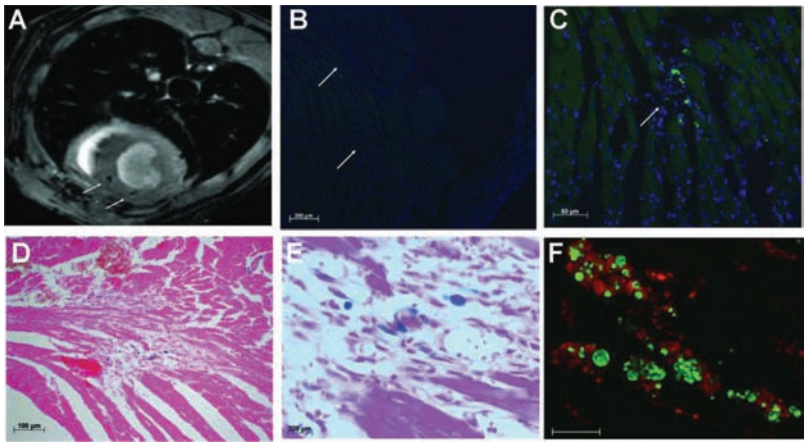

FIG. 7. Localization of MPIO labeled hAFS cells in the live mouse heart by MRI and histology. One million cells were injected in two different locations in the left ventricle of the mouse heart. The mice were scanned by MRI after 14 days (**A**). Cell integration was further confirmed histologically by visualizing MPIOs using fluorescence microscopy (**B** and **C**) and by Prussian blue Iron staining indicating that the labeled cells colocalize with the hypointense region seen by MRI (**D** and **E**). Further, it was confirmed by immunostaining for a human specific nuclear matrix antibody (Anti-NuMA) to prove colocalization of MPIOs with injected AFS cells (scale bar = 10 μm) (**F**).

Stem cells capable of differentiating to multiple lineages may be valuable for therapy. We reported the isolation of human amniotic fluid-derived stem (AFS) cells that express embryonic and adult stem cell markers. Undifferentiated AFS cells expand extensively without feeders, double in 36 hours, and are not tumorigenic. Clonal human lines can be induced to differentiate into cell types representing each embryonic germ layer [18]. The cardiac therapeutic potential for hAFS is not understood yet, however we are evaluating it at this time. The focus of this study was to evaluate noninvasive MRI tracking of labeled hAFS in the mouse heart in order to use this technology in our future cardiac and other organ studies. We demonstrated that MPIO labeling of hAFS cells does not significantly affect proliferation or differentiation. Further we demonstrated that a significant and detectable preparation of hAFS cells are maintained labeled for up to 4 weeks. Our results agree with previous studies showing that other types of cells readily incorporate MPIOs and that their function is not compromised [11,20–22].

Over the past years, other methods of labeling and tracking stem cells have been used. Nanometer-sized ultra-small dextran-coated iron particles (USPIOs) have been used commonly to affect MRI signal intensities. However, one disadvantage of using USPIOs is the fact that a cell must incorporate millions of USPIOs in order to have enough iron within the cell body to generate a detectable decrease in signal in a T2* weighted image. As the cell divides, it and its daughters each retain only some of the iron, and after several cell divisions, none of the cells have enough iron within them to be detectable in the MR image. One possible solution to this problem is to use particles that are large enough so that single particles appear easily in MRI [10]. Iron oxide is a superparamagnetic material that distorts the magnetic field in its presence. The resulting inhomogeneity in the magnetic field can cause a localized decrease in signal in a T2* weighted MR image, provided that enough iron is present and the resolution of the MRI is high enough that the decrease is not washed out by the other signal in the voxel. The main advantage of using iron oxide to label cells is that the effect on the surrounding magnetic field extends well beyond the iron oxide itself on the order of 50 times its size [10,12]. Because of this, individual micron sized iron oxide particles can be detected in MR images. This ensures that no matter how many cell divisions occur, at least some daughter cells will retain enough iron to be detected in MR images. Nanoparticles, on the other hand, can be spread out during cell division into concentrations that are too small to be detected in MR images. It is generally accepted that it will be difficult to distinguish regions of hypointensity that are due to the presence of iron in cells from regions of hypointensity that are due to other causes such as background. Previously, it has been reported that MPIO labeled cells that died upon transplantation produce a less intense and grainy contrast, making it easy to distinguish from the noise-like signal profiles of free particles [23]. In our study, the hypointense regions caused by the labeled cells were clearly identifiable and easily discerned from the relatively homogeneous myocardial tissue.

The ability to successfully track labeled cells in the live mouse heart using MRI represents improvements in spatial resolution and gating/triggering protocol. There have been limited studies using labeled stem cells in the hearts of small animals [24]. In our study, the identification and tracking of MPIO-labeled hAFS cells in the beating hearts of live mice required the elimination of motion artifacts associated with respiratory (~50 breaths/min under anesthesia) and cardiac motion (~375–450 beats/min under anesthesia). The elimination of motion artifacts was achieved by triggering MRI acquisition on the R-wave peak of the electrocardiogram (ECG) waveform and by stopping data acquisition during breaths. Several technical problems had to be solved in order for the triggering to function properly. The Radio Frequency (RF) pulses that generate the signal for the MR image also created noise in the ECG waveform that is received by the computer that monitors vital signs. The selection of a pulse sequence that was fast enough to allow the setting of TR to be less than 85% of the length of the cardiac cycle ensured that the subsequent R-wave peak was not obscured by noise. However, the noise caused by the RF could still generate false trigger signals during the first part of the cardiac cycle. Therefore, the monitoring/triggering program was set to not look for a peak in the ECG waveform for a length of time that was 5 to 10 ms less than the length of the cardiac cycle. This prevented the RF noise in the ECG signal from initiating a false trigger during the RF pulse sequence. Our 7T field

strength and 400 mT/m gradient coil strength allowed us to achieve in plane resolution of 117 × 156 μm. This was on the order of the spatial resolution reported to be necessary for the in vivo identification of MPIO-labeled hAFS cells [11,12].

Quantification of the size/volume of the hypointense regions of the mice injected with labeled stem cells showed that the measured volumes of the hypointense region associated with the labeled cells did not change significantly during the 4 weeks of the study. Quantification of the average intensity of the hypointense regions over time of the mice showed that the average intensity of the hypointense regions did not change significantly during the 4 weeks of the study. These results suggest that in vivo delivery of cells may lead to limited proliferation in contrast to continuous proliferation as shown in vitro (Fig. 3). There may be two possible mechanisms to explain this finding. One, the injected cells could be lacking proliferation inductive signals from the tissue in contrast to the rich in vitro environment. On the other hand, the in vivo environment may provide differentiation signals which could lead to terminal differentiation of the cells and growth arrest. Taken together, this data demonstrates that we can image labeled stem cells over time, as well as a possibility to quantify the amount of stem cells present at various times based on the hypointensity volumes. We are currently studying the correlation between the hypointensity volumes and cell numbers over time.

In conclusion, our results indicate that hAFS cells can be successfully labeled with micrometer sized iron particles (MPIOs) without affecting proliferation and differentiation, maintain labeled up to 4 weeks, and can be noninvasively tracked longitudinally in the mouse heart by a 7.0T MRI. This technique could provide biologic insight into stem cell homing and engraftment in the heart as well as other organs such as neurological stem cells in the brain tissue [25], homing of stem cells to specific organs [26], and tumor therapies [27]. We are currently investigating tracking MPIO-labeled hAFS cells after intravenous injection in the ischemic myocardium. Our results from this study further confirms recently published work by Ebert et al. where they noninvasively tracked embryonic stem cells using MPIOs in the mouse heart [22]. Developing methods for non-invasively tracking and monitoring stem cells in vivo will be of great importance for the future of clinical applications in cell therapy.

Acknowledgments

This research was supported, in part, by an NIH Ruth L. Kirschstein National Research Service Award Individual Fellowship (F31) (#AA016056-01) (D.M.D), a predoctoral fellowship from Fundacao para Ciencia e Tecnologia, Portugal (SFRH/BD/11802/2003) (P.M.B), NC Biotechnology Center, 2005-IDG-1012 (J.Z.), DOD US Army, C033645 (J.Z.). We would like to thank Dr. Kerry Link and the Center for Biomolecular Imaging for providing scan time on the 7.0T MRI scanner. We would also like to thank Dr. J. Koudy Williams for critically reviewing the manuscript.

References

1. Orlic D, J Kajstura, S Chimenti, I Jakoniuk, SM Anderson, B Li, J Pickel, R McKay, B Nadal-Ginard, DM Bodine, A Leri and P Anversa. (2001). Bone marrow cells regenerate infarcted myocardium. Nature 410:701–705.
2. Toma C, MF Pittenger, KS Cahill, BJ Byrne and PD Kessler. (2002). Human mesenchymal stem cells differentiate to a cardiomyocyte phenotype in the adult murine heart. Circulation 105:93–98.
3. Pozzilli P, C Pozzilli, P Pantano, M Negri, D Andreani and AG Cudworth. (1983). Tracking of indium-111-oxine labelled lymphocytes in autoimmune thyroid disease. Clin Endocrinol (Oxf) 19:111–116.
4. Zhou R, DH Thomas, H Qiao, HS Bal, SR Choi, A Alavi, VA Ferrari, HF Kung and PD Acton. (2005). In vivo detection of stem cells grafted in infarcted rat myocardium. J Nucl Med 46:816–822.
5. Hofmann M, KC Wollert, GP Meyer, A Menke, L Arseniev, B Hertenstein, A Ganser, WH Knapp and H Drexler. (2005). Monitoring of bone marrow cell homing into the infarcted human myocardium. Circulation 111:2198–2202.
6. Zhou R, DH Thomas, H Qiao, HS Bal, SR Choi, A Alavi, VA Ferrari, HF Kung and PD Acton. (2005). In vivo detection of stem cells grafted in infarcted rat myocardium. J Nucl Med 46:816–822.
7. Lanza GM, DR Abendschein, X Yu, PM Winter, KK Karukstis, MJ Scott, RW Fuhrhop, DE Scherrer and SA Wickline. (2002). Molecular imaging and targeted drug delivery with a novel, ligand-directed paramagnetic nanoparticle technology. Acad Radiol 9(Suppl. 2):S330–S331.
8. Massoud TF and SS Gambhir. (2003). Molecular imaging in living subjects: seeing fundamental biological processes in a new light. Genes Dev 17:545–580.
9. Bulte JW, ID Duncan and JA Frank. (2002). In vivo magnetic resonance tracking of magnetically labeled cells after transplantation. J Cereb Blood Flow Metab 22:899–907.
10. Hinds KA, JM Hill, EM Shapiro, MO Laukkanen, AC Silva, CA Combs, TR Varney, RS Balaban, AP Koretsky and CE Dunbar. (2003). Highly efficient endosomal labeling of progenitor and stem cells with large magnetic particles allows magnetic resonance imaging of single cells. Blood 102:867–872.
11. Shapiro EM, S Skrtic, K Sharer, JM Hill, CE Dunbar and AP Koretsky. (2004). MRI detection of single particles for cellular imaging. Proc Natl Acad Sci USA 101:10901–10906.
12. Shapiro EM, S Skrtic and AP Koretsky. (2005). Sizing it up: cellular MRI using micron-sized iron oxide particles. Magn Reson Med 53:329–338.
13. Kraitchman DL, AW Heldman, E Atalar, LC Amado, BJ Martin, MF Pittenger, JM Hare and JW Bulte. (2003). In vivo magnetic resonance imaging of mesenchymal stem cells in myocardial infarction. Circulation 107:2290–2293.
14. Hill JM, AJ Dick, VK Raman, RB Thompson, ZX Yu, KA Hinds, BS Pessanha, MA Guttman, TR Varney, BJ Martin, CE Dunbar, ER McVeigh and RJ Lederman. (2003). Serial cardiac magnetic resonance imaging of injected mesenchymal stem cells. Circulation 108:1009–1014.
15. Arai T, T Kofidis, JW Bulte, J de Bruin, RD Venook, GJ Berry, MV Mcconnell, T Quertermous, RC Robbins and PC Yang. (2006). Dual in vivo magnetic resonance evaluation of magnetically labeled mouse embryonic stem cells and cardiac function at 1.5 t. Magn Reson Med 55:203–209.
16. Himes N, JY Min, R Lee, C Brown, J Shea, X Huang, YF Xiao, JP Morgan, D Burstein and P Oettgen. (2004). In vivo MRI of embryonic stem cells in a mouse model of myocardial infarction. Magn Reson Med 52:1214–1219.
17. Kustermann E, W Roell, M Breitbach, S Wecker, D Wiedermann, C Buehrle, A Welz, J Hescheler, BK Fleischmann and M Hoehn. (2005). Stem cell implantation in ischemic mouse heart: a high-resolution magnetic resonance imaging investigation. NMR Biomed 18:362–370.

18. De Coppi P, G Bartsch Jr., MM Siddiqui, T Xu, CC Santos, L Perin, G Mostoslavsky, AC Serre, EY Snyder, JJ Yoo, ME Furth, S Soker and A Atala. (2007). Isolation of amniotic stem cell lines with potential for therapy. Nat Biotech 25:100–106.
19. Lee G, H Kim, Y Elkabetz, G Al Shamy, G Panagiotakos, T Barberi, V Tabar and L Studer. (2007). Isolation and directed differentiation of neural crest stem cells derived from human embryonic stem cells. Nat Biotechnol 25:1468–1475.
20. Frank JA, BR Miller, AS Arbab, HA Zywicke, EK Jordan, BK Lewis, LH Bryant Jr. and JW Bulte. (2003). Clinically applicable labeling of mammalian and stem cells by combining superparamagnetic iron oxides and transfection agents. Radiology 228:480–487.
21. Zhao M, MF Kircher, L Josephson and R Weissleder. (2002). Differential conjugation of Tat peptide to superparamagnetic nanoparticles and its effect on cellular uptake. Bioconjug Chem 13:840–844.
22. Ebert SN, DG Taylor, HL Nguyen, DP Kodack, RJ Beyers, Y Xu, Z Yang and BA French. (2007). Noninvasive tracking of cardiac embryonic stem cells in vivo using magnetic resonance imaging techniques. Stem Cells 25:2936–2944.
23. Shapiro EM, K Sharer, S Skrtic and AP Koretsky. (2006). In vivo detection of single cells by MRI. Magn Reson Med 55:242–249.
24. Tallheden T, U Nannmark, M Lorentzon, O Rakotonirainy, B Soussi, F Waagstein, A Jeppsson, E Sjogren-Jansson, A Lindahl and E Omerovic. (2006). In vivo MR imaging of magnetically labeled human embryonic stem cells. Life Sci 79:999–1006.
25. Bulte JW, T Douglas, B Witwer, SC Zhang, E Strable, BK Lewis, H Zywicke, B Miller, P van Gelderen, BM Moskowitz, ID Duncan and JA Frank. (2001). Magnetodendrimers allow endosomal magnetic labeling and in vivo tracking of stem cells. Nat Biotechnol 19:1141–1147.
26. Shyu WC, CP Chen, SZ Lin, YJ Lee and H Li. (2007). Efficient tracking of non-iron-labeled mesenchymal stem cells with serial MRI in chronic stroke rats. Stroke 38:367–374.
27. Tang Y, K Shah, SM Messerli, E Snyder, X Breakefield and R Weissleder. (2003). In vivo tracking of neural progenitor cell migration to glioblastomas. Hum Gene Ther 14:1247–1254.

Address reprint requests to:
Shay Soker
Wake Forest University Health Sciences
Medical Center Blvd.
Winston-Salem, NC 27157

Email: ssoker@wfubmc.edu

Received for publication January 29, 2008; accepted after revision March 11, 2008.